35th Annual International Conference of the IEEE EMBS
Osaka, Japan, 3 - 7 July, 2013

Cardiac Right Ventricular Segmentation via Point Correspondence

Kumaradevan Punithakumar*‡, Michelle Noga*‡, and Pierre Boulanger†‡

*Department of Radiology & Diagnostic Imaging, University of Alberta, AB, Canada
†Department of Computing Science, University of Alberta, AB, Canada
‡Servier Virtual Cardiac Centre, Mazankowski Alberta Heart Institute, AB, Canada

***Abstract*—This study presents an approach to the segmentation of the right ventricle (RV) from a sequence of cardiac magnetic resonance (MR) images. Automatic delineation of the RV is difficult because of its complex morphology, thin and ill-defined borders, and the photometric similarities between the connected cardiac regions such as papillary muscles and heart wall. Further, geometric/photometric models are hard to build from a finite training set because of the significant differences in size, shape, and intensity between subjects. In this study, we propose to use a non-rigid registration method developed recently to obtain the point correspondence in a sequence of cine MR images. Given the segmentation on the first frame, the proposed method segments both endocardial and epicardial borders of the RV using the obtained point correspondence, and relaxes the need of a training set. The proposed method is evaluated quantitatively on common data set by comparison with manual segmentation, which demonstrated competitive results in comparison with recent methods.**

I. Introduction

Assessment of right ventricular (RV) function and volume is important in the diagnosis of cardiovascular diseases [1]. Clinical measurements such as the RV ejection fraction (EF) and volumes have important diagnostic, prognostic, and therapeutic implications in patients with acquired heart disease who need cardiac function follow-up [2], [3]. Magnetic resonance (MR) imaging allows an exhaustive RV evaluation with high spatial resolution, and provides a large number of images. MR imaging has several important advantages over echocardiography, including excellent image quality and lack of geometric assumptions. For quantitative functional analysis and to obtain clinical measurements such as EF, it is essential to delineate the RV. Manual delineation of the RV boundary in all MR images[1] is tedious and time-consuming, and automating the process has been the subject of an intense research effort recently [4].

Due to its complex morphology and function, assessment of the RV is acknowledged as a more challenging problem than the assessment of the left ventricle. The problem becomes more difficult due to thin and ill-defined RV borders, its crescent shaped structure, and the complex deformations of the RV chamber. Further, the RV segmentation methods should also consider the photometric similarities between the connected cardiac regions, for instance, the papillary muscles and heart wall have approximately the same intensity. Therefore, standard segmentation methods based solely on intensity information cannot yield accurate tracking. To overcome these difficulties, most of the existing methods use atlas-based techniques [5], [6] or prior geometric properties [7], [8], such as the shape of the RV learned *a priori* from a finite-training set. If only shapes similar to the training set are allowed, the use of active shape and appearance models can lead to a realistic solution. However, the optimization of such models does not always guarantee the global optima. The main drawbacks of statistical shape or atlas based approaches are the requirement of large manually segmented training sets and the results highly dependent on the choice of the training data. The results are often biased towards a particular cardiac pathology.

Further, the shape of the RV is significantly different at end-systole in comparison to end-diastole. Therefore, in general, it is more difficult to obtain a good segmentation of the RV at end-systole than at end-diastole using the shape-based approaches. The results published by the recent RV segmentation challenge at the MICCAI 2012 conference show that most of the existing methods have the highest segmentation error at end-systole. The best reported Dice metric (DM) values among the seven participants were 0.72 and 0.77 for endocardium and epicardium, respectively. Due to its smaller size, inaccuracies in the segmentation of the RV at end-systole affect the clinical measurements such as EF significantly.

To tackle the problem of delineation of the RV, we propose to use point correspondence using a non-rigid registration method developed recently [9]. Given the segmentation of the first frame, the proposed method segments both endocardial and epicardial borders of the RV using the obtained point correspondence. The proposed method has several advantages over existing ones: (1) a shape prior is not needed to obtain satisfying RV segmentations because the point correspondence can track any curve in the image sequence; (2) the distributions of intensity or shape data is not assumed and the method relaxes the need of a training set; (3) the method is more flexible for congenital heart disease where the RV is more variable in shape. Using registration to delineate the RV is advantageous in that it provides the sequence of corresponding points over time, a useful attribute in many cardiac applications such as wall motion analysis. Further, the proposed method allows RV volumetric analysis over the complete cardiac cycle, and the automatic detection of end-systolic and end-diastolic phases as it provides segmentation at each step in the cycle.

The proposed method is evaluated quantitatively over 32 subjects on a common data set by comparison with manual segmentations, and yielded average Dice scores of 0.79 and 0.84, respectively, for endocardial and epicardial seg-

[1]Typically, the number of images per subject is equal to 200.

978-1-4577-0216-7/13/$26.00 ©2013 IEEE

mentations, a competitive result in comparison with current methods.

II. Methods

We use a points correspondence between the first image T_1 and k^{th} image T_k defined over $\Omega \subset \mathbb{R}^2$ to obtain a sequence of points over time. It can be formulated as the optimization of similarity/dissimilarity measure [9].

$$\hat{\phi} = \arg\operatorname*{opt}_{\phi} E_s(T_1, T_k, \phi(\xi)) \tag{1}$$

for each pixel location $\xi \in \Omega$, where $\phi : \Omega \to \Omega$ is a transformation function, and $E_s(\cdot)$ a measure of similarity. As this problem may not have a unique solution, we introduce a deformation field using a Jacobian transformation μ and curl of end velocity field γ, where $\mu : \Omega \to \mathbb{R}$ and $\gamma : \Omega \to \mathbb{R}$

1) Moving Mesh Generation: Let $\mu(\xi)$ be a continuous monitor function constrained by

$$\int_{\Omega} \mu = |\Omega|, \tag{2}$$

The purpose of this step is to find a transformation $\phi : \Omega \to \Omega, \partial\Omega \to \partial\Omega$, so that

$$J_{\phi}(\xi) = \mu(\xi), \tag{3}$$

where J_{ϕ} denotes the transformation Jacobian. The following computations yield a transformation ϕ which verifies (3).
Step 1: Compute a vector field $\rho(\xi)$ which verifies

$$\operatorname{div} \rho(\xi) = \mu(\xi) - 1 \tag{4}$$

Step 2: Build a velocity vector field from $\rho(\xi)$:

$$\nu_t(\xi) = \frac{\rho(\xi)}{t + (1-t)\mu(\xi)}, \qquad t \in [0,1], \tag{5}$$

where t is an artificially introduced (algorithmic) time.
Step 3: Finally, ϕ is obtained by solving the following ODE:

$$\frac{d\psi(\xi,t)}{dt} = \nu_t(\psi(\xi,t)), \qquad t \in [0,1], \psi(\xi, t=0) = \xi, \tag{6}$$

and setting ϕ equal to ψ evaluated at $t = 1$: $\phi(\xi) = \psi(\xi, t = 1)$.

We add an additional constraint on the curl of $\rho(\xi)$ to (4) and solve the ensuing div-curl system under the Dirichlet boundary condition to obtain a unique solution, as the above problem may have multiple solutions, i.e.,

$$\begin{cases} \operatorname{div} \rho(\xi) = \mu(\xi) - 1 & \text{(7a)} \\ \operatorname{curl} \rho(\xi) = \gamma(\xi) & \text{(7b)} \end{cases}$$

with null boundary condition $\rho(\xi) = 0 \forall \xi \in \partial\Omega$, where $\gamma(\xi)$ is a continuous function over Ω. Hence, the transformation can be fully parametrized by $J_{\phi}(\xi)$ and $\gamma(\xi)$. We ensure the uniqueness of the solution using the Dirichlet boundary condition [10]. The Dirichlet boundary conditions may cause the motion errors to be high at the image boundaries and, therefore, we pad both images by zeroes.

With the above parametrization, we reformulate (1) as the following constrained optimization problem [9]:

Problem: Given two images T_1 and T_k, defined over Ω, find the function pair $\{\mu(\xi), \gamma(\xi)\}$, that optimizes the cost in (1)*, subject to:*

$$\begin{cases} \displaystyle\int_{\Omega} \mu(\xi) d\xi = |\Omega| & \text{(8a)} \\ \tau_h > \mu(\xi) > \tau_l, \qquad \xi \in \Omega' \subset \Omega & \text{(8b)} \end{cases}$$

where $0 < \tau_l$ ensuring that $\phi_{\mu,\gamma}$ is a diffeomorphism, and Ω' is a sub-region of image domain Ω.

Constraints (8a) and (8b) ensures the areas of the domain and co-domain are equal after transformation and enforces the *incompressibility* constraint in sub-region Ω', respectively. Note that a diffeomorphism corresponds to a positive transformation Jacobian, which is enforced explicitly via the monitor function [11].

The above problem can be solved by a *step-then-correct* optimization strategy. We refer the reader to [9] for derivation and numerical implementation details. We compute a sequence of corresponding points on endocardial as well as epicardial borders in all the frames using transformation function $\hat{\phi}$, given the segmentation on the first frame.

III. Experiment

The proposed method was evaluated over the Training and Test1 sets provided by the RV segmentation challenge[2], MICCAI 2012. Each data set consists of short-axis MRI volumes of 16 subjects. The data sets were acquired on 1.5T MR scanners (Symphony Tim, Siemens Medical Systems, Erlangen, Germany) with steady-state free precession acquisition mode. More details about the data can be found at the RV segmentation challenge website. The following parameter values were used for all cases: $\tau_h = 4$ and $\tau_l = 0.25$. Ground truth manual segmentations were provided only for the Training set. In order to assess the performance of the proposed algorithm on the Test1 Set, we submitted the automatic contours to the RVSC organizers, who in return, provided us with the performance measures.

A. Statistical performance evaluation

Two criteria were used to evaluate the similarities between the manual segmentations and the automatic segmentations:

1) The DM: We computed the DM, a common measure of similarity between manual and automatic segmentation. The DM is given by

$$DM(V_a, V_m) = \frac{2V_{am}}{V_a + V_m} \tag{9}$$

where V_a , V_m, and V_{am} are the volumes of the automatically segmented region, the corresponding manually delineated region, and the intersection between them, respectively. Note that DM is always between 0 and 1, where 1 means a perfect match.

[2]http://www.litislab.eu/rvsc/

2) The Hausdorff distance (HD): We computed the HD [12], a symmetric measure of distance between both automatic and manual contours. Let us denote automatic and manual contours by C_a and C_m, respectively. For each point p_a^i on C_a, we compute the distances to all the points p_m^j on C_m. The HD is given by

$$HD(C_a, C_m) = \max(\max_i(\min_j(d(p_a^i, p_m^j))), \max_j(\min_i(d(p_a^i, p_m^j)))) \quad (10)$$

where $d(\cdot)$ is the Euclidean distance. The HD is computed in mm with spatial resolution obtained from the PixelSpacing in the DICOM header.

Table I reports the DM and HD values for Training and Test1 sets. The proposed method yielded average Dice scores of 0.79 and 0.84, respectively, for endocardial and epicardial segmentations. The average DM values for endocardium and epicardium for each subject in the Training and Test1 sets are depicted in Fig. 3(a) and (b). The figure demonstrates that the proposed method yielded high conformance with manual segmentations in most cases.

We also evaluated the performance of the proposed method for estimating the clinical measurements, end-systolic volume (ESV) and the EF. We did not report end-diastolic volume since it corresponds to the manual segmentation. Table II reports the correlation coefficient R and coefficients of linear regression fit ($y = ax + b$) for ESV and EF estimation. The proposed method yielded high correlation between manual and automatic clinical measurements. Linear regression plots of ESV and EF, depicted in Fig. 2(a) and (b) with the identity line, illustrate this correlation. The average and standard deviation errors between automatic and manual EF are 0.0858 ± 0.06 and 0.1874 ± 0.13 for Training and Test1 sets, respectively.

TABLE I. MEAN AND STANDARD DEVIATION OF DICE METRIC (DM) AND HAUSDORFF DISTANCE (HD) BETWEEN THE PROPOSED SEGMENTATION AND MANUAL DELINEATION AT THE END-SYSTOLE.

	Dice metric	Hausdorff distance (mm)
Training Set		
Endocardium	0.8168 ± 0.15	7.07 ± 4.03
Epicardium	0.8627 ± 0.10	7.53 ± 3.73
Test1 Set		
Endocardium	0.7676 ± 0.16	9.64 ± 4.15
Epicardium	0.8220 ± 0.10	9.99 ± 3.85

TABLE II. CORRELATION COEFFICIENT R AND COEFFICIENTS OF LINEAR REGRESSION FIT ($y = ax + b$) BETWEEN THE PROPOSED METHOD AND GROUND TRUTH.

Measurement	Linear regression coefficients
Training Set	
ESV	$R = 0.9929, a = 1.0102, b = 3.7846$
EF	$R = 0.9611, a = 0.9229, b = 0.0047$
Test1 Set	
ESV	$R = 0.9834, a = 0.9602, b = 19.1602$
EF	$R = 0.9263, a = 0.7937, b = 0.0306$

Fig. 1. Representative example of segmented endocardial (green) and epicardial (yellow) borders of the RV over a complete cardiac cycle.

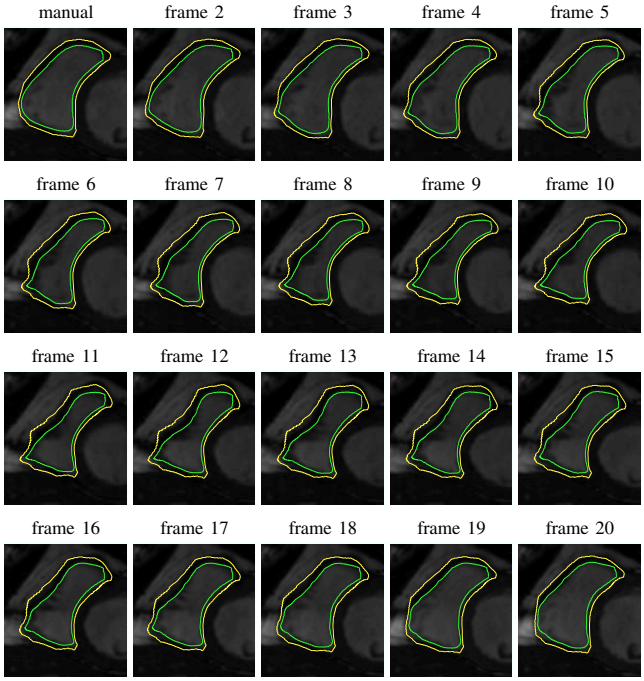

B. Visual Inspection

In Fig. 1, we give representative examples of segmented endocardial and epicardial borders of the RV over a complete cardiac cycle. These examples show that the proposed method accurately included the papillary muscles inside the target cavity, although these have similar intensity profile to the RV myocardium.

The proposed method allows RV volumetric analysis over the complete cardiac cycle. Fig 4 shows the volume of the RV cavity plotted against time step, where we applied Simpson's rule in computing the volumes based on the segmented RV areas and slice spacing.

Our MATLAB parallel implementation of the proposed algorithm running on two quad-core 2.4 GHz Intel Xeon processors took 5.85 ± 2.10 seconds to process a sequence of 19 images.

IV. CONCLUSION

This study presents an approach to segment the RV from short-axis cine MR sequences. The proposed approach

Fig. 2. Comparisons of manual and automatic segmentations over 16 subjects from the Training set. (a) Automatic versus manual end-systolic volumes. The proposed method obtained a high correlation coefficient of $R = 0.9929$ (b) Automatic versus manual ejection fractions. The proposed method obtained a correlation coefficient of $R = 0.9611$.

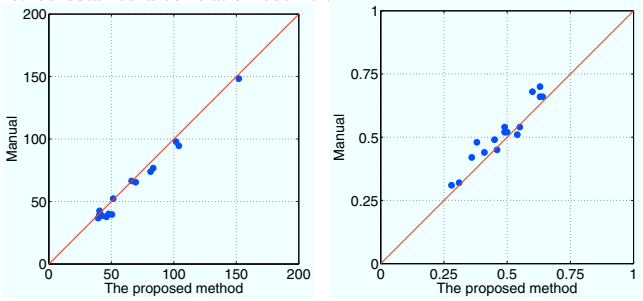

(a) ES volume (b) Ejection fraction

Fig. 3. Average Dice scores for endocardium and epicardium for each subject in the Training and Test1 sets at end-systole.

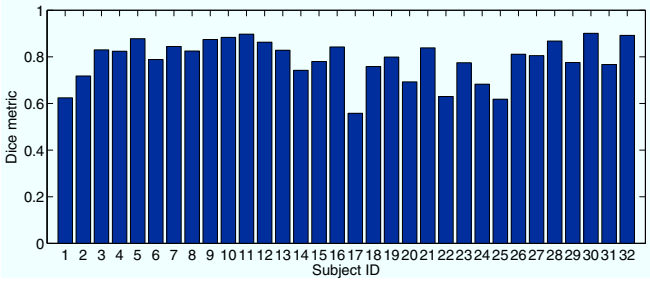

(a) Endocardium

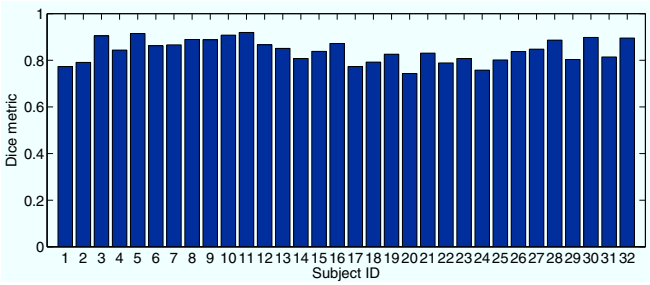

(b) Epicardium

Fig. 4. A representative example of the RV endocardial volume curve computed using the proposed approach. We applied Simpson's rule in computing the volumes using segmented RV areas and slice spacing.

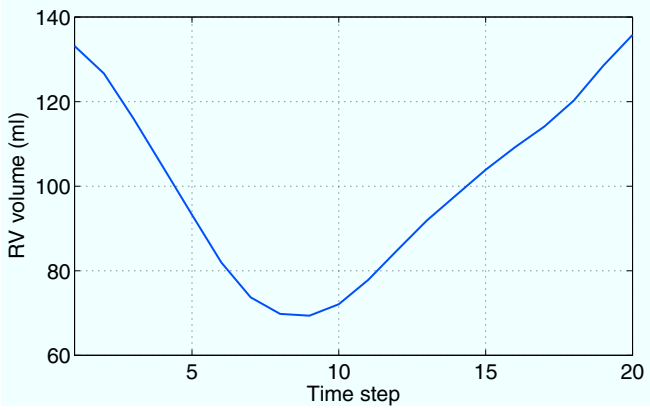

is based on point correspondence between the sequence of images computed using a recent nonlinear registration algorithm. Given the segmentation on the first frame, the proposed method segments both endocardial and epicardial borders of the RV, and does not require a training data set. The proposed method is evaluated quantitatively over 32 subject on a common data set by comparison with manual segmentations, and yielded average Dice scores of 0.79 and 0.84, respectively, for endocardial and epicardial segmentations, a competitive result in comparison with related recent methods.

V. Acknowledgment

Authors wish to thank Servier Canada Inc. for the grant which supported this work.

References

[1] J. Caudron, J. Fares, V. Lefebvre, P.-H. Vivier, C. Petitjean, and J.-N. Dacher, "Cardiac MRI assessment of right ventricular function in acquired heart disease: Factors of variability," *Academic Radiology*, vol. 19, no. 8, pp. 991 – 1002, 2012.

[2] S. Ghio, A. Gavazzi, C. Campana, C. Inserra, C. Klersy, R. Sebastiani, E. Arbustini, F. Recusani, and L. Tavazzi, "Independent and additive prognostic value of right ventricular systolic function and pulmonary artery pressure in patients with chronic heart failure," *Journal of the American College of Cardiology*, vol. 37, no. 1, pp. 183–188, 2001.

[3] S. R. Mehta, J. W. Eikelboom, M. K. Natarajan, R. Diaz, C. Yi, R. J. Gibbons, and S. Yusuf, "Impact of right ventricular involvement on mortality and morbidity in patients with inferior myocardial infarction1," *Journal of the American College of Cardiology*, vol. 37, no. 1, pp. 37–43, 2001.

[4] C. Petitjean and J.-N. Dacher, "A review of segmentation methods in short axis cardiac MR images," *Medical Image Analysis*, vol. 15, no. 2, pp. 169–184, 2011.

[5] J. Lotjonen, S. Kivisto, J. Koikkalainen, D. Smutek, and K. Lauerma, "Statistical shape model of atria, ventricles and epicardium from short- and long-axis MR images," *Medical Image Analysis*, vol. 8, no. 3, pp. 371–386, September 2004.

[6] M. Lorenzo-Valdes, G. I. Sanchez-Ortiz, A. G. Elkington, R. H. Mohiaddin, and D. Rueckert, "Segmentation of 4D cardiac MR images using a probabilistic atlas and the EM algorithm," *Medical Image Analysis*, vol. 8, no. 3, pp. 255 – 265, 2004.

[7] S. Mitchell, B. Lelieveldt, R. van der Geest, H. Bosch, J. Reiver, and M. Sonka, "Multistage hybrid active appearance model matching: segmentation of left and right ventricles in cardiac MR images," *Medical Imaging, IEEE Transactions on*, vol. 20, no. 5, pp. 415 – 423, may 2001.

[8] S. Ordas, L. Boisrobert, M. Huguet, and A. Frangi, "Active shape models with invariant optimal features (IOF-ASM) application to cardiac MRI segmentation," in *Computers in Cardiology*, vol. 30, 2003, pp. 633–636.

[9] H.-m. Chen, A. Goela, G. J. Garvin, and S. Li, "A parameterization of deformation fields for diffeomorphic image registration and its application to myocardial delineation," in *MICCAI 2010*, ser. LNCS, T. Jiang *et al.*, Eds., vol. 6361. Springer, 2010, pp. 340–348.

[10] X. Zhou, "On uniqueness theorem of a vector function." *Progress in Electromagnetics Research*, vol. 65, pp. 93–102, 2006.

[11] J. Liu, "New development of the deformation method," Ph.D. dissertation, Department of Mathematics, The University of Texas at Arlington, 2006.

[12] D. Huttenlocher, G. Klanderman, and W. Rucklidge, "Comparing images using the Hausdorff distance," *Pattern Analysis and Machine Intelligence, IEEE Transactions on*, vol. 15, no. 9, pp. 850 –863, sep 1993.